CONF-9209290--3

INTERNATIONAL ATOMIC ENERGY AGENCY

FOURTEENTH INTERNATIONAL CONFERENCE ON PLASMA PHYSICS AND CONTROLLED NUCLEAR FUSION RESEARCH

Würzburg, Germany, 30 September – 7 October 1992

IAEA-CN-56/A-7-16

PPPL-CFP--2764

DE93 006154

Particle and Energy Transport Studies on TFTR and Implications for Helium Ash in Future Fusion Devices

E.J. SYNAKOWSKI, P.C. EFTHIMION, G. REWOLDT, B.C. STRATTON, W.M. TANG, R.E. BELL, B. GREK, R.A. HULSE, D.W. JOHNSON, K.W. HILL, D. K. MANSFIELD, D. McCUNE, D.R. MIKKELSEN, H.K. PARK, A.T. RAMSEY, S.D. SCOTT, G. TAYLOR, J. TIMBERLAKE, M.C. ZARNSTORFF

Princeton Plasma Physics Laboratory
Princeton University
Princeton, New Jersey 08543
United States of America

1. INTRODUCTION

Particle and energy transport in tokamak plasmas have long been subjects of vigorous investigation. Present-day measurement techniques permit radially resolved studies of the transport of electron perturbations [1], low- and high-Z impurities [2,3,4,5], and energy [6,7,8,9]. In addition, developments in transport theory [10] provide tools that can be brought to bear on transport issues. Here, we examine local particle transport measurements of electrons, fully-stripped thermal helium, and helium-like iron in balanced-injection L-mode and enhanced confinement (Supershot [11]) deuterium plasmas on TFTR of the same plasma current, toroidal field, and auxiliary heating power. He^{2+} and Fe^{24+} transport has been studied with charge exchange recombination spectroscopy (CHERS) [12,13], while electron transport has been studied by analyzing the perturbed electron flux following the same helium puff used for the He^{2+} studies. By examining the electron and He^{2+} responses following the same gas puff in the same plasmas, an unambiguous comparison of the transport of the two species has been made. The local energy transport has been examined with power balance analysis, allowing for comparisons to the local thermal fluxes. Some particle and energy transport results from the Supershot have been compared to a transport model based on a quasilinear picture of electrostatic toroidal drift-type microinstabilities [10]. Finally, implications for future fusion reactors of the observed correlation between thermal transport and helium particle transport is discussed.

2. THE EXPERIMENT, RESULTS, AND COMPARISON TO THEORY

The toroidal field B_T of these plasmas was 4.8 T, the plasma current I_p was 1.0-1.1 MA, and the balanced-injection neutral beam heating power was 12-13 MW. The major radius was 2.45 m, and the minor radius was 0.8 m. Differences in the plasmas were found in the electron temperature T_e, ion temperature T_i, electron density n_e and peakedness $n_e(0)/\langle n_e \rangle$ of the electron density profile, and energy confinement time as measured by magnetics (for the L-mode, $\tau_E = 60$ ms $= 1.0 x \tau_E^{L\text{-mode}}$; for the Supershot, $\tau_E = 150$ ms $= 2.5 x \tau_E^{L\text{-mode}}$ for plasmas with helium puffs, 160 ms for plasmas with iron injection). Typical plasma profiles, obtained during the neutral beam heated phase of the discharge and mapped to minor radius, are shown in Fig. 1. $T_e(r)$ was measured using both Thomson scattering and a grating polychromator. $T_i(r)$ was measured by CHERS, viewing the 5292 Å line of C^{5+} (n=8-7). The central Z_{eff} was typically 3.1 - 3.3 in the Supershot and 1.5 in the L-Mode. $Z_{eff}(r)$ was measured both with a tangentially viewing visible bremsstrahlung (VB) array and with radial profiles of C^{6+}, normalized to the central beam stopping cross sections, charge exchange rates for the three beam species, and electron impact excitation rates relevant to plume brightness calculations.

For all perturbations, it is assumed that the flux can be represented as the sum of diffusive and convective flows, i.e.

$$\Gamma = -D\nabla n + Vn \quad (1)$$

for each species. For He^{2+} and Fe^{24+}, transport coefficients are interpreted as those of trace particles and thus representative of steady-state values. For electrons, however, the perturbed flux is from electrons introduced by the gas puff and possibly from a perturbation in the flux of the background electrons due to small changes in the transport coefficients. Thus the relationship between the steady-state coefficients and the perturbative values depends strongly on the underlying transport mechanisms [1,17]. Profiles of diffusivities of all density perturbations for the three species are shown in Fig. 3(a-c) for both the L-mode and Supershot. All are radially hollow and typically 1-2 orders of magnitude larger than neoclassical values [18] throughout the plasma cross section, except possibly at the magnetic axis. For $r/a < 0.4$, D_{He} is smaller in the Supershot than in the L-Mode. This fact suggests that, if the helium transport is similar to the thermal deuterium transport, one local characteristic of improved particle confinement in the Supershot is reduced ion particle diffusivity as compared to the L-Mode. Important to note is that D_{Fe} is actually *larger* in the Supershot than in the L-Mode, and D_e does not necessarily equal D_{He}, although they come from the same perturbation. These observations underscore the point that particle transport of a given plasma is not necessarily characterized well by a single species. In addition, the fact that the impurity diffusivities are on the order of or larger than D_e indicates that no present theory of transport induced by magnetic stochasticity can account for the bulk of anomalous particle transport in TFTR, although a subdominant role cannot be ruled out.

Using measured radial profiles of plasma parameters including n_e, T_e, T_i, and Z_{eff}, and the calculated beam energy deposition, thermal heat fluxes Q_i of the ions and Q_e of the electrons were evaluated using the transport code TRANSP [19,20]. We define the single fluid effective thermal conductivity χ_{fluid} as

$$Q_e + Q_i \equiv -\chi_{fluid}(n_e\nabla T_e + \sum_j n_j \nabla T_i) \quad (2)$$

where the sum is over the thermal ion species. Changes in χ_{fluid} between L-Mode and Supershot are similar to changes in D_{He} (Fig. 3). This characteristic of χ_{fluid} is driven by the measured relationship between D_{He}, V_{He}, and χ_{fluid}, assuming a fixed edge helium density.

In the limit where the heat flux Q is from alpha particle heating alone, the assumption that the slowing-down alpha particles do not diffuse leads to an ash source profile shape that is similar to that of the heating source profile. In steady-state, $-\nabla\cdot\Gamma_{He} = S_{He}$, where S_{He} is the thermal alpha source. The heat source is given by $E_\alpha S_{He}$, where E_α is the alpha energy of 3.5 MeV, and $-\nabla\cdot Q = E_\alpha S_{He}$. For steady state, relating the two equations of continuity yields

$$\frac{dn_{He}}{dr} - \frac{V_{He}}{D_{He}} n_{He} = - n_e \frac{\chi_{fluid}}{E_\alpha D_{He}} \frac{dT}{dr} \quad (3)$$

If the helium transport is dominated by diffusion and if the density profile is flat, then an expression valid for all shapes of D_{He} and χ_{fluid} but constant χ_{fluid}/D_{He} implies $n_{He}(r)/n_e(r) \cong \chi_{fluid}T(r)/(D_{He}/E_\alpha) + n_{He}(a)/n_e(r)$. This simple expression underscores the importance of the relation between local heat transport and helium particle transport. If T = 30 keV, $n_e(0) = 1.35\times10^{20}$ m^{-3}, and the edge helium density $n_{He}(a) = 0.01n_e(0)$ (required for proper divertor pumping [23]), considerations based on magnetic stochasticity give $\chi_{fluid}/D_{He} \approx \sqrt{m_{He}/m_e} = 85$. This yields enormous helium concentrations of 70%, clearly incompatible with sustained ignition. However, if $\chi_{fluid}/D_{He} \sim 1$, typical of the values found here for the Supershot and L-Mode, expected helium concentrations are about 2%.

This picture is complicated by the fact that $V_{He} \neq 0$ in some plasmas, as was clearly seen for r/a < 0.5 in the Supershot. We investigate the role of convection by solving eq. (3) using plasma profiles similar to those used in Ref. 23 for an ignited ITER plasma (r = 3.1 m, T(0) = 30 keV, $n_e(0) = 1.35\times10^{20}$ m^{-3}, $\langle n_e\rangle = 1.2\times10^{20}$ m^{-3}, Z_{eff} from carbon = 1.4). An edge helium density of $0.1n_e(a)$ was assumed. Results obtained with the nominal bulk plasma values (r/a < 0.8) of V_{He}/D_{He} as a function of r/a measured in the L-Mode and for the Supershot are shown in fig. 4. It was assumed that $\chi_{fluid}/D_{He} \sim 3$, a value at the bounds of the experimental uncertainties. The L-Mode transport coefficients lead to a helium profile that is quite broad. Central helium concentrations are about 8%, consistent with sustained ignition at these densities and temperatures [Ref. 23]. While the helium profiles obtained using the Supershot V_{He}/D_{He} are strongly peaked, this occurs in a region of small plasma volume, leading to a relatively small decrease in fusion power of about 10%. This indicates inward convection of the type observed in the Supershot is compatible with sustained ignition. Of course, generalizations should be viewed with caution until a

[20] GOLDSTON, R.J. et al., J. Comp. Phys. **43** (1981) 161.

[21] ENGELMANN, F., NOCENTINE, A., Comments Plasma Phys. Controlled Fusion **5** (1980) 253.

[22] TAYLOR, R.J., FRIED, B.D., MORALES, G.J., Comments Plasma Phys. Controlled Fusion **13** (1990) 227.

[23] REDI, M.H., COHEN, S.A., SYNAKOWSKI, E.J., Nucl. Fusion **31** (1991) 1689.

[24] HILLIS, D.L., FINKEN, K.H., HOGAN, J.T., *et al.*, Phys. Rev. Lett. **65** (1990) 2382.

Fig. 1. Plasma profiles for the L-Mode and Supershot mapped to minor radius and measured during the electron density flattop during neutral beam injection. a) Electron density n_e. b) Electron temperature T_e and ion temperature T_i.

Fig. 2. a). Steady-state He^{2+} density profile shapes measured 150 ms after the gas puff for the L-Mode and Supershot. The profiles are normalized where the scale lengths are similar. b). He^{2+} concentrations, normalized to the plasma edge for clarity. Uncertainties are from systematic errors common to both measurements, making the changes in profile shape more certain than the profile shape itself. Included are ±15 % uncertaintes in the beam stopping cross section, electron impact excitation and ionization rates of helium plumes, and charge exchange excitation rates.

Fig. 3. Transport coefficients for L-Mode and Supershot. a). Helium diffusivity b). Iron diffusivity. c). Perturbative electron diffusivity. d). Single fluid thermal conductivity.

Fig. 4. Simulated helium density profiles for ITER using core values ($r/a < 0.8$) of V_{He}/D_{He} from the L-Mode and Supershot. The electron density shown and central temperature of 30 keV was assumed. For both cases, $\chi_{fluid}(r)/D_{He}(r) = 3$.

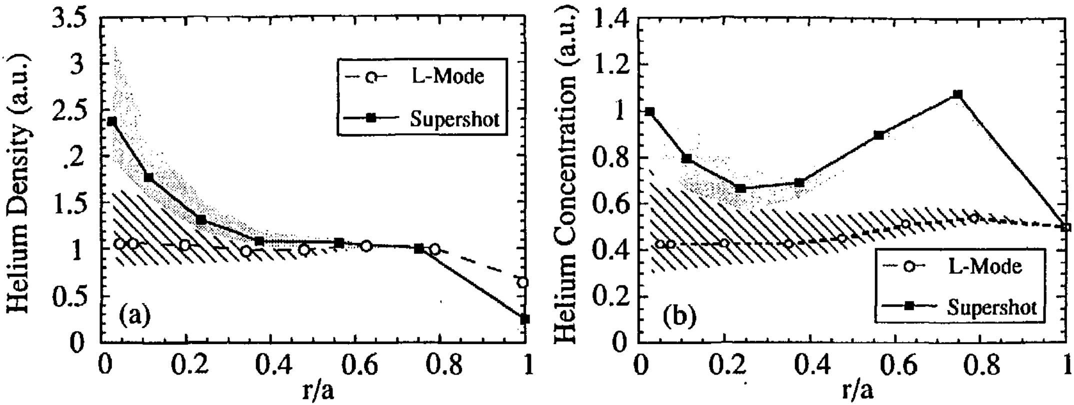

Helium Density (a.u.)
3.5
3
2.5
2
1.5
1
0.5
0
0
0.2
0.4
0.6
0.8
1
r/a
L-Mode
Supershot
(a)
Helium Concentration (a.u.)
1.4
1.2
1
0.8
0.6
0.4
0.2
0
0
0.2
0.4
0.6
0.8
1
r/a
L-Mode
Supershot
(b)

Fig. 2

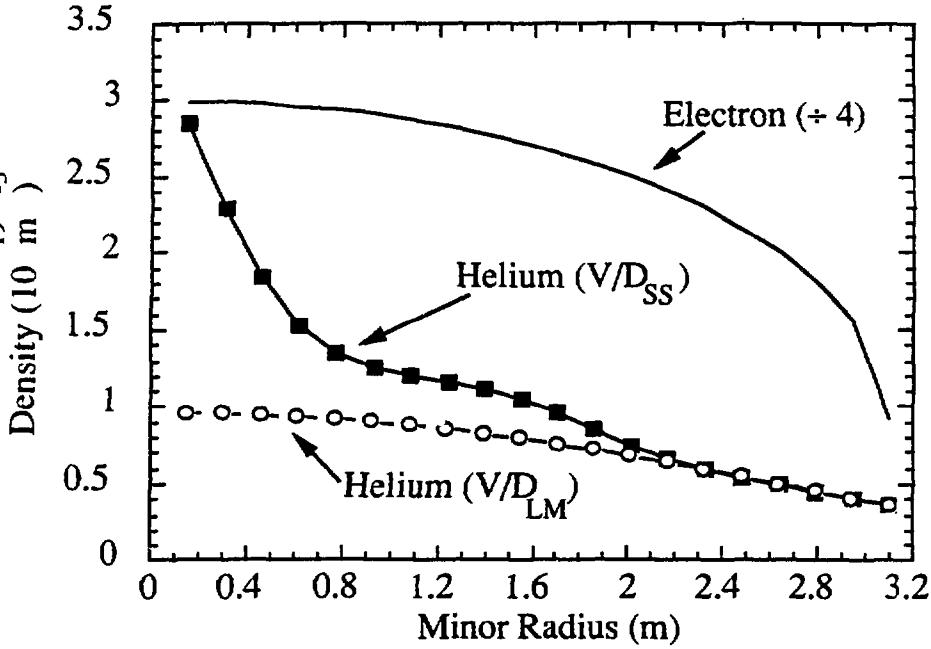
Density (10^19 m^-3)
3.5
3
2.5
2
1.5
1
0.5
0
Electron (÷ 4)
Helium (V/D_SS)
Helium (V/D_LM)
0
0.4
0.8
1.2
1.6
2
2.4
2.8
3.2
Minor Radius (m)

Fig. 4